Application of the optical transform to the electron diffraction pattern of polyethylene single crystal

Akiyoshi Kawaguchi
Institute for Chemical Research, Kyoto University, Uji, Kyoto 611 *Japan*
(*Received* 3 *April* 1980; *revised* 30 *June* 1980)

The setting angle of the planar zigzag molecular chains in a polyethylene single crystal has been determined by optical transformation of the electron diffraction pattern, using the Patterson synthesis. The reproducibility of the original structure on optical transformation was confirmed by (1) the inverse optical transform of the optical diffraction pattern produced by a well defined two-dimensional model lattice and (2) the electron diffraction pattern calculated from the model crystal. The following points arising from the electron diffraction were examined: the dynamical scattering, multiple reflections and radiation damage of the specimen; the direction of the interatomic vector obtained by the present method of analysis and under these illumination conditions was found to be reliable. The optical results were confirmed by X-ray diffraction in which these effects were absent.

INTRODUCTION

When polyethylene crystallizes from dilute solution, a single crystal with lozenge-shaped lamellae is formed where the molecular chains are normal to the lamellar surface and the chains fold back and forth many times. Studies of the conformation of folded-chain molecules which are characteristic of the lamella, and, in particular, studies of folds on the lamallar surface, have been carried out and several models have been proposed in order to meet energetic and geometric requirements[1-5]. The above works were based on the crystal structure of polyethylene as analysed by Bunn[6]. Since his first analysis, several investigations into the crystal structure have been carried out[7-10]. However, no work on the single crystal is found until our first study on the application of the optical transform to the electron diffraction pattern of the single crystal[11], although the experimental determination of the crystal structure of a single crystal is still needed in order to proceed with the conformation analysis of the fold.

The application of the optical transform method to structural investigations has been developed largely by Lipson and others[12-14] and has been widely used to study crystal structures. Use of a computer enables the crystal structure analysis to be undertaken in a routine manner. However, the structure can be visualized as an image with this method which, in principle, remains an excellent and straightforward method for the structure analysis. The advantages of the method are shown to the full in image processing by optical filtering[15]. Here, we focus on the direct analysis of the setting angle of polyethylene molecules in the single crystal from the optical transform of the electron diffraction pattern. Details of the method are described and some interesting points are examined.

EXPERIMENTAL

Sample

Single crystals of unfractionated linear polyethylene (Sholex 6050) were prepared isothermally from the 0.05 wt % solution in *p*-xylene at 80°C. Electron micrographs (*Figure 1*) show a multilayered lamellar crystal resulting from the spiral growth. The lamellar thickness was estimated at ~120 Å from the small-angle X-ray scattering measurement of sedimented mats of single crystals.

Electron diffraction and intensity measurement

The electron diffraction pattern (*ED* pattern) from a multilayer crystal was taken with a 500 kV high voltage electron microscope. The multiple exposure method was

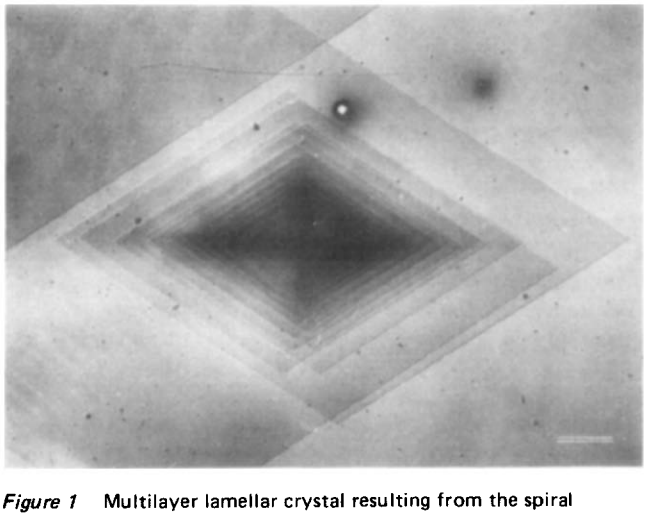

Figure 1 Multilayer lamellar crystal resulting from the spiral growth. Scale bar, 1 μm

0032-3861/81/060753-09$02.00

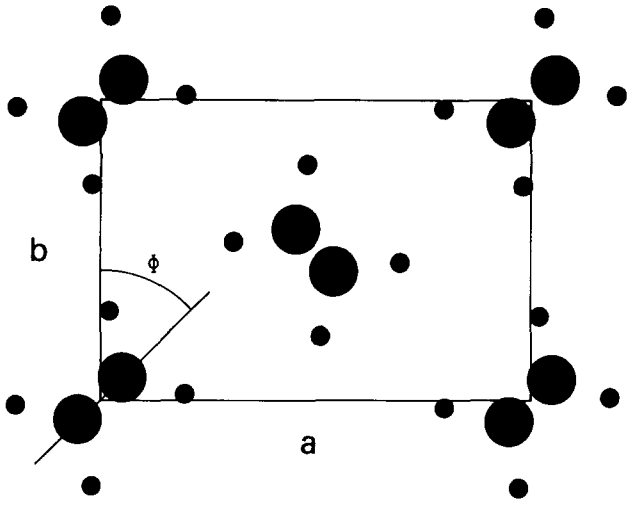

Figure 2 Projection of the unit cell of polyethylene crystal on the basal plane (001). Large and small solid circles represent the carbon and hydrogen atoms, respectively. The angle Φ between the b-axis and the projection of planar zigzag molecular chains is defined as the setting angle. Values of *a* and *b* measured in the present work as 7.43 Å and 4.93 Å respectively

adopted in order to cover a wide range of diffraction intensities; i.e. a series of electron diffraction photographs were taken for various exposure times. A large series of photographs were taken and those in which the ED patterns were most symmetrical were selected (*Figure 4a*). The integrated intensities of the diffraction spots were measured photometrically using the integration method wherever the slits of a microphotometer were sufficiently wide as to cover the spots completely. Since single crystals are composed of large numbers of small crystallites with slightly different orientations, the mosaic character must be taken into account in the evaluation of the relative intensities of the reflections. According to Vainshtein[16], the correction of this angular distribution of crystallites in space can be made by introducing an angular factor (the Lorentz factor), $d(hkl)/\alpha$, where $d(hkl)$ denotes the lattice spacing of (hkl) plane and α denotes the effective angular distribution of crystallites. After making this intensity correction, all the diffraction patterns could be standardized so that the intensities of diffraction spots with moderate intensity (for example 020 reflection) were set to be equal. By averaging the intensities of the corresponding diffraction spots of these normalized patterns, one symmetrical diffration pattern together with its reflection intensities were obtained.

Method of analysis

The crystal structure (or the molecule) can be visualized by the use of the Fourier synthesis in the form of an image or a map. However, two serious problems arise in this synthesis from the electron diffraction data. Firstly, some ambiguity is inevitable in deriving the moduli of the structure amplitudes from the reflection intensities, mainly because of the dynamical interaction of electron waves, even when the intensities are accurately measured. Secondly, the phase angles of the structure amplitudes cannot be determined only from the experimental data. Since the Patterson synthesis (i.e. the Fourier transform of the reflection intensities) is independent of the phase problem, this synthesis may be carried out using experimental data only, and hence this method was used for our studies. The Patterson pattern is the self-convolution of the crystal structure or the molecular image and the pattern itself is a complicated assembly of interatomic vectors. Accordingly, the image quality suffers due to some deterioration, while the effect of the dynamical scattering on the image is considerably reduced and the interatomic vectors are correctly represented by peaks[17]. Here, the direction of interatomic vectors, such as the setting angle of polyethylene molecules in the crystal (*Figure 2*), is of primary importance and the Patterson synthesis fits for the present purpose of our investigation.

The present investigation was carried out using two different methods: (1) the optical transform method, based on the Patterson synthesis of the *ED* pattern and (2) the standard X-ray diffraction method for a crystal powder. The second method was utilized to confirm the results achieved by the first. The experimental and theoretical details of the optical transform have been reviewed[12], but this method suffers from the serious disadvantage that the difference of phase angle between the diffracting units cannot be introduced. This is another reason why the Patterson synthesis without phase relation was utilized here. In the diffraction pattern of the nickel phthalocyanine crystal which contains a heavy nickel atom, the phase angle is the same for all reflections. The optical transform in this case yields the molecular image[18]. However, since the phase angle of each reflection is different, the structure analysis must usually be carried out through the Patterson synthesis.

Apparatus

The optical system consists of three parts (*Figure 3*): (1) an illumination source which produces parallel beams (a He–Ne gas laser with wavelength 6328 Å); (2) a lens system to focus diffracted beams (a telephoto-lens); and (3) a camera as a recording system for the final image. The masks for the optical transformation were made by photographic reduction of the original patterns and drawings. The mask size was 5 × 5 mm. Other experimental details are noted in Taylor and Lipson[12].

X-ray diffraction measurements

Since lamellar single crystals were slightly oriented in the mats, the mats were crushed and ground into powder at liquid nitrogen temperature to prevent the crystals from distorting. The diffraction intensities of the powder were measured with a scintillation counter by means of the step scanning method with the fixed time mode. The X-ray diffraction measurement was carried out using Ni-filtered CuKα radiation.

RESULTS

Setting angle of polyethylene in the single crystal

All *hk*0 reflections within 1.34 $Å^{-1}$ in the reciprocal space are seen in the *ED* pattern (*Figure 4a*) of the lozenge-

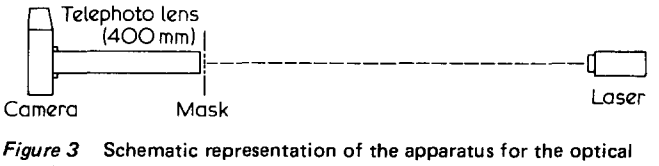

Figure 3 Schematic representation of the apparatus for the optical transform

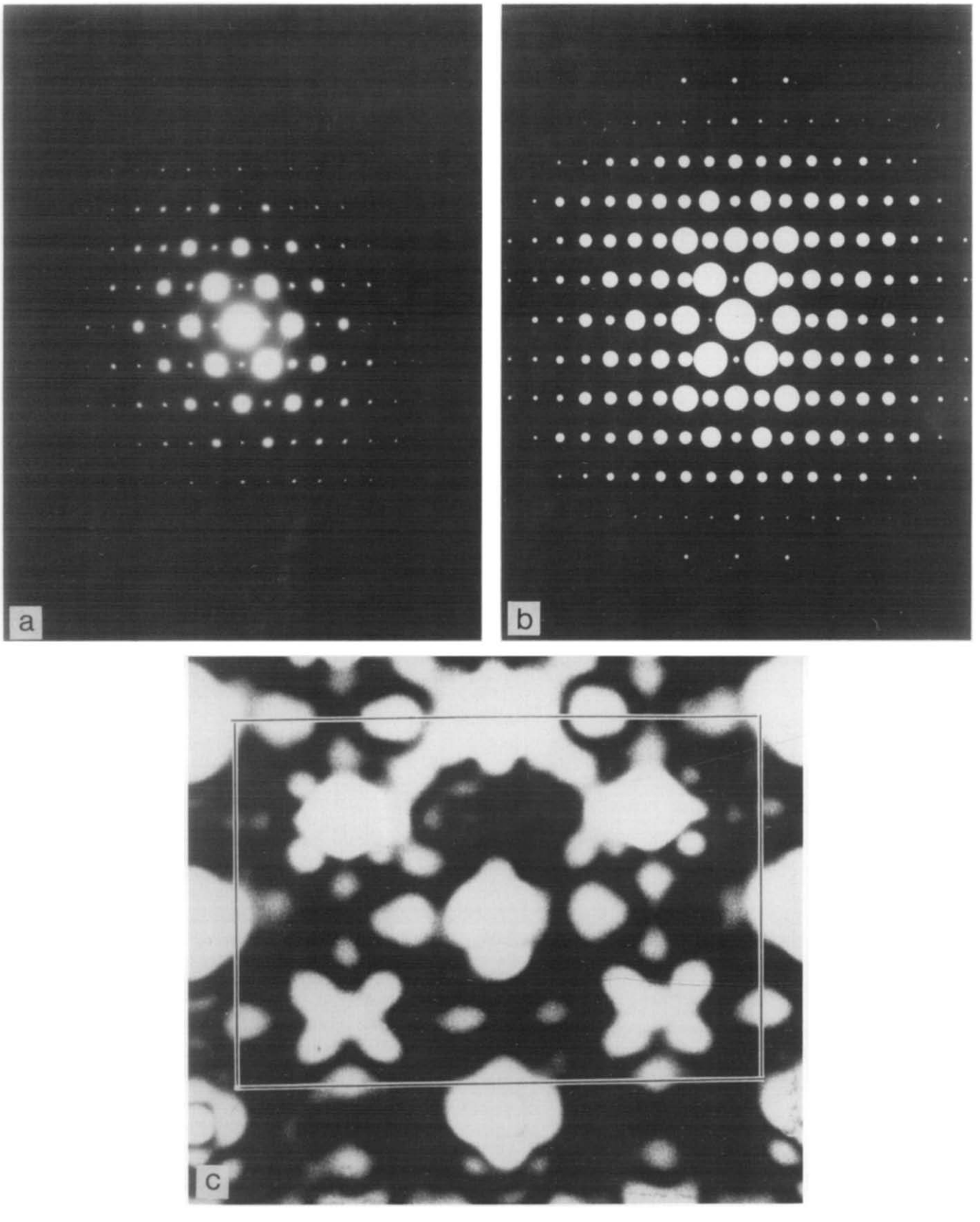

Figure 4 (a) Electron diffraction pattern of the single crystal; (b) schematic electron diffraction pattern drawn on the basis of photometric data according to the text from (a); and (c) the optical transform from the mark of (b)

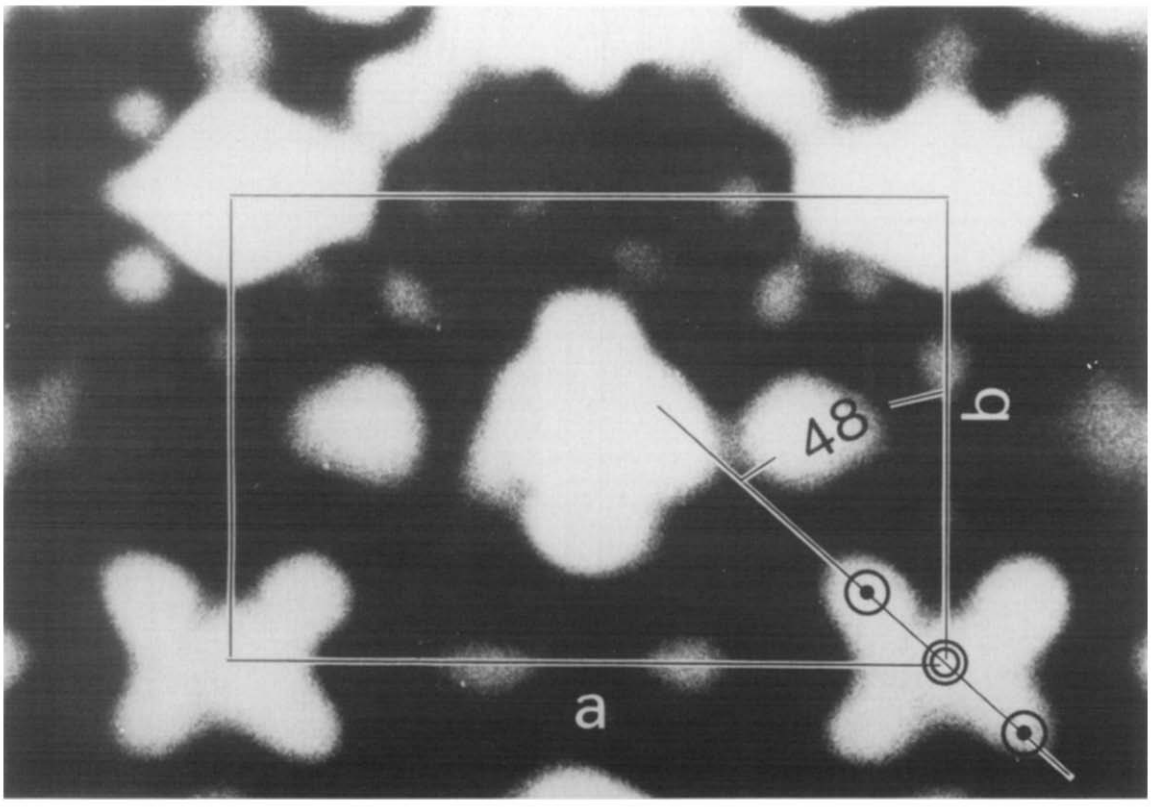

Figure 5 Magnified image of the area enclosed by the rectangle in *Figure 4(c)*

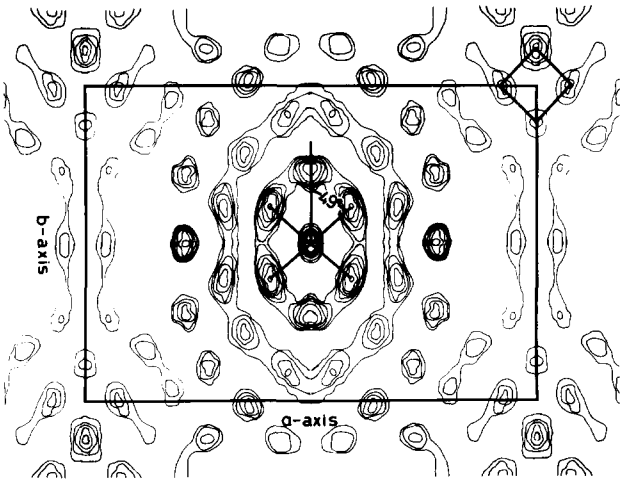

Figure 6 Sharpened Patterson pattern constructed with computer

shaped single crystals grown from dilute solution. According to the law of extinction, the reflections of Miller indices ($h00$) and ($0k0$) are forbidden in the polyethylene crystal when h and k are odd. However, these reflections appear with an observable intensity in the diffraction pattern recorded. The original *ED* pattern was redrawn on the basis of the measured data in such a manner that the radius of each disc representing the diffraction spot is proportional to the square root of diffraction intensity (*Figure 4b*). This pattern was optically transformed after reduction into the mask and the transform is shown in *Figure 4c*. The image formed corresponds to the two-dimensional Patterson map projected on the basal plane, i.e. the self-convolution of polyethylene crystal projected on the plane in the direction of the molecular axis. Since polyethylene crystal is composed only of carbon and

Table 1 Results obtained by the X-ray diffraction analysis

	Atomic coordinates		
Atom	x	y	z
C	0.046	0.064	0.25
H–1	0.201	0.051	0.25
H–2	−0.001	0.295	0.25

	Observed and calculated structure factors	
(hkl)	$\lvert F_{obs}\rvert$	$\lvert F_{cal}\rvert$
110	14.7	15.4
200	13.1	14.1
210	2.8	3.2
020	7.7	7.6
120	2.7	2.8
011	6.0	5.3
310	5.2	4.6
111	4.2	3.3
201	6.4	5.3
220	4.0	3.6
211	3.5	3.0
400	3.9	3.8
311	3.5	3.8

Setting angle, 47.1°
Isotropic temperature factor, 5.2 Å^{-2}
Reliability factor, 8%

hydrogen atoms, the peaks in the pattern become more marked for the superposed carbon–carbon atomic pair. An example of an interatomic vector is shown in *Figure 5* by the vector between two intense peaks marked with open circles. This vector is equivalent to the projection of a C–C vector of a planar zigzag molecular chain on the (001) basal plane of a unit cell in the direction of the molecular axis. The setting angle is given by the angle

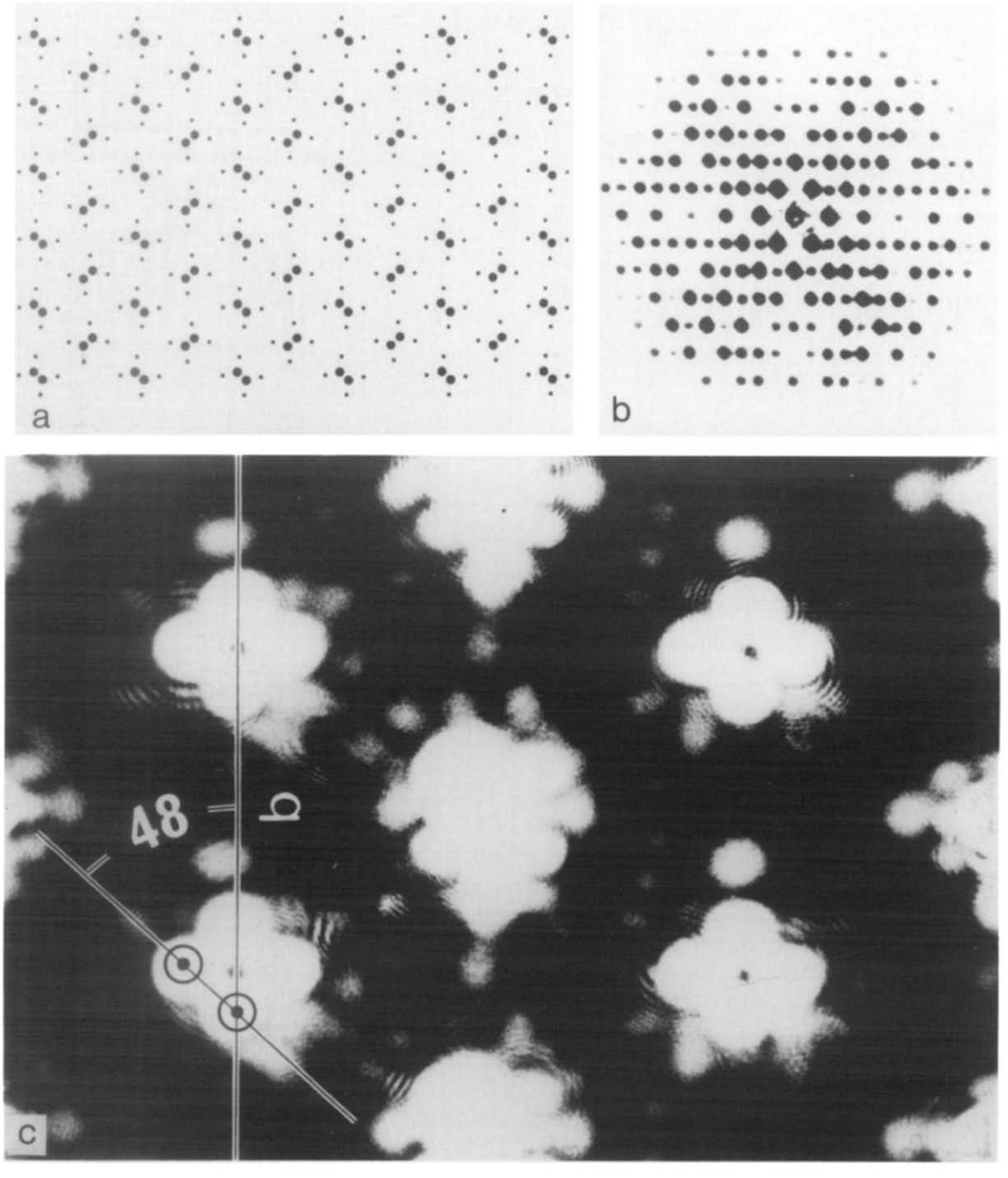

Figure 7 Two-dimensional model lattice of the projected polyethylene lattice with setting angle 48°. The large and small discs represent carbon and hydrogen atoms, respectively. *a*-axis is horizontal and the *b*-axis vertical. (b) Optical diffraction pattern produced by the mask of (a); (c) The optical transform of the optical diffraction pattern (b)

between this vector and the *b*-axis of unit cell and is estimated at 48° from *Figure 5*.

The forbidden reflections observed in *Figure 4a* are ghosts with regard to the original crystal structure, so that the optical transform may reproduce a false structure when the diffraction pattern including these forbidden reflections are optically transformed. However, the exclusion of these reflections from the diffraction pattern made no difference to the result of its optical transform and hence it is concluded that the forbidden ghost reflections have no influence on the optical transform.

Figure 6 shows the sharpened Patterson pattern constructed using the photometric intensity data with the computer. The X and diamond shapes characteristic of the Patterson pattern based on the atomic arrangement of the unit cell of *Figure 2* are clearly seen. These are also seen in *Figure 5*. In this construction, the function $\exp(-Bs^2)$ was used as a weighting function in order to sharpen the peaks of the Patterson pattern and enhance the resolution. Here, $s=\sin\theta/\lambda$ where θ and λ denote the Bragg angle and the wavelength, respectively. B was set at $10\,\text{Å}^{-2}$ which corresponds to twice the temperature factor (see *Table 1*). The setting angle is estimated from this pattern at 49° which agrees well with the result from the optical transform. This agreement shows that the selection of disc sizes representing the diffraction spots, which is of primary importance in order to reproduce a good optical transform, was appropriate in the present pro-

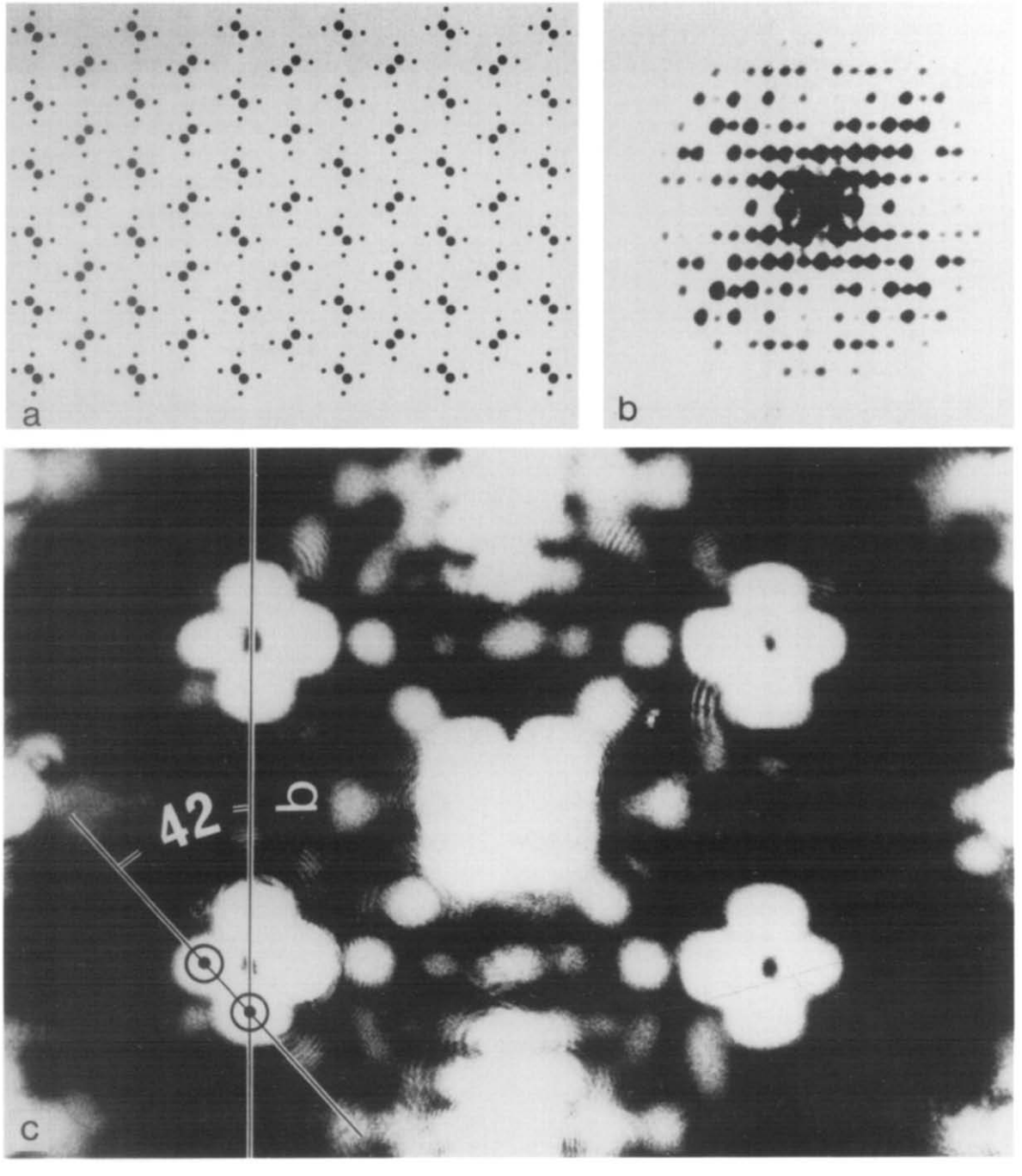

Figure 8 (a) Model lattice with the setting angle 42°; (b) its optical diffraction pattern; and (c) the optical transform produced from (b)

cedure, e.g. the radius of disc for the strongest reflection was 100 μm.

Optical transform of the 'optical diffraction pattern' of a two-dimensional model lattice

The reliability of the optical method may be examined by the inverse optical transform of the optical diffraction pattern produced from the well-defined two-dimensional model lattice. The two-dimensional model lattices in *Figures 7a* and *8a* correspond to the models for the projection of a polyethylene lattice on the basal plane (001), where carbon and hydrogen atoms are represented by the discs with diameters proportional to the scattering factor of each atom at $s=0$. In these models, the usual bond angles and bond lengths were assumed: $<CCC = 109°26'$, $<HCH = 110°$, $l_{CC} = 1.54$ Å and $l_{CH} = 1.1$ Å. The setting angle is 48° in the first model (*Figure 7a*) and 42° in the second model (*Figure 8a*) as estimated in the present work and by Bunn respectively. The optical diffraction patterns were produced from the masks made of these models (*Figures 7b* and *8b*) and then optically transformed (*Figures 7c* and *8c*). The images in *Figures 7c* and *8c* correspond to the Patterson images of *Figures 7a* and *8a*. The setting angles estimated from these images are 48° and 42° which are exactly equal to those set in the original model lattices. Therefore, it has been shown that this optical method based on the Patterson synthesis is a useful, reliable and reproducible method in determining the magnitude of a fine angle such as the setting angle.

Optical transform of calculated electron diffraction pattern

The optical transform is formed from the electron

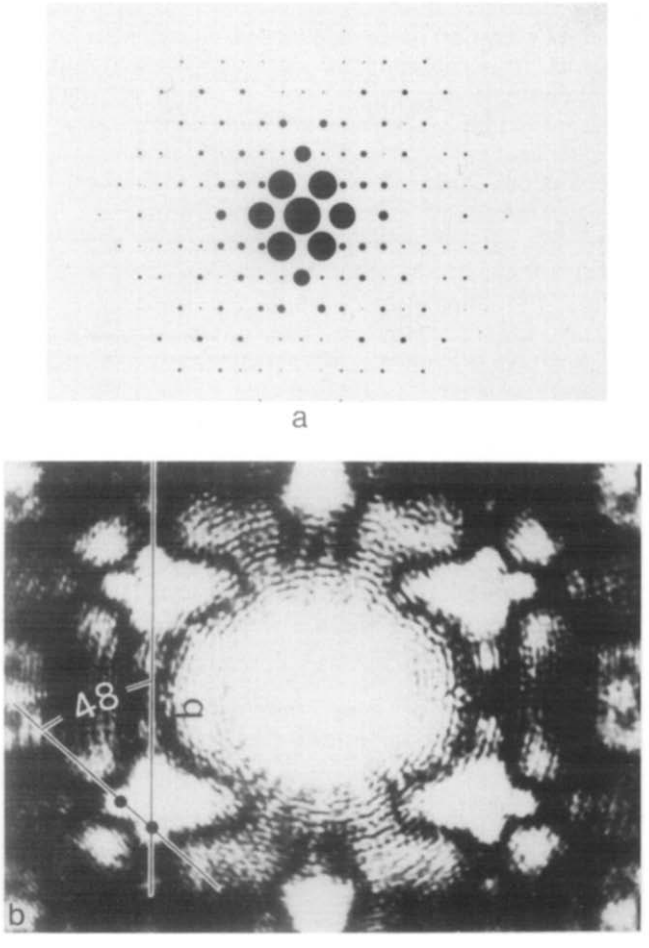

Figure 9 (a) Schematic electron diffraction pattern drawn on the basis of the structure amplitudes calculated on the model lattice of *Figure 7* (a); and (b) its optical transform

diffraction pattern corresponding to a two-wavelength microscope with no phase correlation. Since the light scattered by a disc and the electrons scattered by an atom behave in different ways, the optical diffraction pattern of the model lattice differs from the electron diffraction pattern of real polyethylene crystal (compare *Figure 4a* with *Figures 7b* and *8b*). The discrepancy between the two patterns is more marked for the higher order reflections. This difference may indicate that the optical transform does not reproduce the original structure with high fidelity. The following procedure was an attempt to ensure the validity of the optical transform of the *ED* pattern. The *ED* pattern was artifically made where the radii of the diffraction spots were proportional to the moduli of the structure amplitudes calculated from the ideal polyethylene crystal lattice. *Figure 9a* shows the *ED* pattern obtained from the model lattice of *Figure 7a*. The pattern was optically transformed (*Figure 9b*) and the setting angle was found to be 48°. In the case of a 42° setting angle good reproducibility was also achieved. Thus it is concluded that the setting angle can be determined accurately even with the two-wavelength microscope from the *ED* pattern.

X-ray diffraction analysis

The intensities of the diffraction peaks were obtained from their profile analysis on the basis of the curve analysis proposed by Hindeleh and Johnson[19]. Correction for Lorentz polarization and absorption was made for the observed intensities. Since the diffraction pattern was the Debye–Scherrer pattern, only reflections which were singly indexed were used for the structure analysis. The refinement of the crystal structure was carried out by the least squares method[9,10] and *Table 1* shows the results. The setting angle thus obtained agrees well with that by the above optical transform process.

DISCUSSION

The Patterson image, i.e. the optical transform of an electron diffraction pattern, was found to be useful for the analysis of an unknown structure. For example, a reliable value was obtained for the setting angle of polyethylene molecules in the polyethylene crystal. However, in the case of a thick specimen or containing heavy atoms, the electron diffraction should be treated dynamically because of the effects of multiple scattering of electrons. Structure analysis by the electron diffraction method is not suitable for this kind of specimen and the present optical method may not therefore be applicable. To examine the dynamical effects on the polyethylene crystal, the electron diffraction amplitudes were calculated by the *n*-beam diffraction theory developed by Cowley and Moodie based on physical optics[20]. In this approach, a sample is divided into a certain number of slices and the transmission of electrons through the sample is represented by the transmission through the set of slices, each of which is approximated by the phase grating, i.e. by the Fresnel diffraction. *Figure 10* shows the moduli of struc-

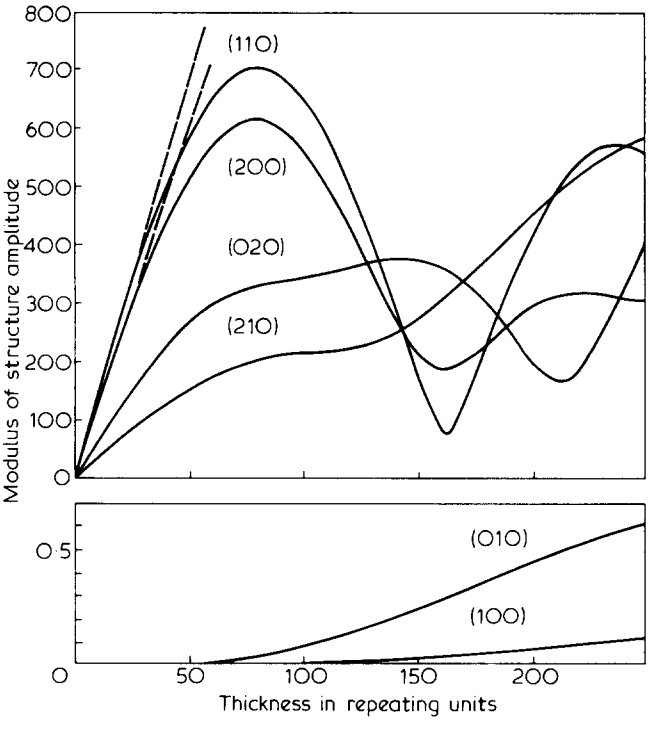

Figure 10 The variation of the moduli of structure amplitudes of (100), (010), (110), (200), (210) and (020) reflections as a function of the crystal thickness. The thickness of slice used in the calculation is equal to the length of the repeating unit in the direction of the *c*-axis, 2.54 Å. The dashed lines show the variation of the moduli of the structure amplitudes for the kinetic diffraction. The calculation was carried out for the example where the incident direction of the electron beam was parallel to the molecular axis

ture amplitudes for four typical reflections of polyethylene crystals as a function of the thickness. It is found from *Figure 10* that the dynamical diffraction amplitudes for the polyethylene lamella with a thickness of 120 Å (about 48 in a repeating unit) decrease by a factor 0.8–0.9 from the kinematical amplitudes. This decrease may not be neglected even in the Patterson synthesis as proposed by Dorset[21]. Holland *et al.* have shown that the diffraction contrast of a dislocated network which was observed in the electron micrograph of a bilayered polyethylene single crystal can be explained by the dynamical diffraction of electrons, and not by the kinematical diffraction[22]. However, since the result of the Patterson synthesis is in good agreement with that of X-ray diffraction then the present method seems to be safe for structural work. It should be noted, however, that this method is safe only for the determination of the direction of interatomic vectors, and not their magnitude, while the magnitude of the present C–C vector measured from *Figure 5* deviates considerably from the value given by X-ray diffraction. Two reasons for this deviation are considered. First, the Patterson image is not so sensitive to the intensity variation when the intensities do not change markedly. Secondly, the comparative magnitude of the intensities among the reflections is maintained, e.g. the intensity relation breaks when the crystal thickness reaches several hundred angstroms.

The above discussion is limited to a single lamella. Since the real specimen is composed of a pile of several lamellae (*Figure 1*), the transmission of electrons is complicated and therefore multiple reflections may occur more often than secondary reflections. Judging from the *ED* pattern of *Figure 4a* and the amplitude variation with the crystal thickness, it can easily be seen that the real electron diffraction pattern for the stacked lamellae is not what is expected for a single crystal with the same thickness as that of the stack. The stack does not behave as a single crystal in electron diffraction. However, the appearance of forbidden reflections in *Figure 4a* shows that multiple reflections do occur. *Figure 10* also shows that the dynamical effects on the intensity of the forbidden reflections for a lamella or the lamellar stack are not as large as the observed intensities would suggest. The pattern may be interpreted as follows: the diffraction patterns produced by all the strong spots in the primary reflection are superimposed on the primary pattern by simple translation in such a way that their origins coincide with the strong primary spots. With this in mind we considered only the effect of secondary reflections on the resultant reflection intensity using the analysis of Vainshtein[16]. It is assumed that the intensity of secondary reflection at a point K due to the primary reflection at H is proportional to the product of the intensity of the primary reflection at H and that of the secondary reflection at a point $K-H$ by the primary reflection at H. Here, the letters H and K denote the Miller indices (hkl). The total intensity of the reflection including the secondary reflections at K is given by the summation over all H:

$$I_K = I'_K + b\sum_H I_H \cdot I_{K-H}$$

where I'_K denotes the intensity of the primary reflection at K and b is the proportionality coefficient. The second term on the right-hand side gives the contribution of the secondary effect to the total intensity. Though the intensity loss due to the production of the secondary $K-H$ reflection is included in I'_K, it is assumed to be small and is therefore neglected in the calculation. The value of b was estimated from the apparent intensity for the forbidden reflections by setting I'_K equal to zero. After this correction for the observed intensities, the intensity of the higher order reflection is smaller. For example, the intensities of the reflections of the 8th order and above along the a axis are extremely small. The optical transform of the corrected *ED* pattern yielded the same setting angle, 48°, although the image was blurred when compared with the original *ED* pattern in *Figure 4c*. Compared with the corrected *ED* pattern, the original *ED* pattern (*Figure 4a*) is boosted for the higher order reflections and its optical transform (*Figure 4c*) corresponds to the sharpened Patterson image. It is therefore not surprising that the setting angles obtained from the optical transforms of both the original and corrected *ED* patterns agree fairly well. It should also be noted that *Figure 7* was constructed using a larger B value than that assumed, which resulted in a much sharpened, corrected *ED* pattern.

The resolution of the image in a microscope is given by the Abbe equation, $K\sin\theta/\lambda$, where K is a constant approximately equal to unity. When the projection of C–C bond on the (001) plane (see *Figure 2*) is resolved, the setting angle can be accurately determined. The projected length of the C–C bond is 0.88 Å and, according to the above theory, the reflections with Bragg angle larger than 5×10^{-3} radian must be included in order to resolve the setting angle. Roughly speaking, this limiting angle corresponds to the 600 and 040 reflections. This is because of the small change in the setting angle which results in a large intensity change of the $h40$ and $h50$ reflections as seen in *Figures 7b* and *8b*. All the above optical transforms were formed by including the reflections at least up to the fifth order in the b axis and then the setting angle is sufficiently accurate from the viewpoint of resolution.

The electron irradiation causes the physicochemical changes of specimens; the temperature rise and the radiation damage. The radiation damage is vital for organic materials including polymers which undergo the chemical and/or sturctural changes. Polyethylene is not exceptional in undergoing the physicochemical changes[23] and an observed large setting angle of 48° may be the result of the structural change caused by the electron irradiation. The setting angle of melt-crystallized polyethylene has been found to increase with temperature and to exceed 48° at temperatures >80°C[9,10]. To prevent the irradiation effects, the *ED* pattern should be taken within a short time with the illumination level as low as possible. However, the total radiation dose is almost invariant since as the time required to record the *ED* pattern with low illumination is fairly long. It seems inevitable that some physicochemical change of the specimen will occur under these conditions. Polyethylene is less sensitive to X-ray radiation and the irradiation effects are therefore negligible. As the setting angle obtained by X-ray diffraction agrees well with that by the electron diffraction, it is suggested that the present large setting angle 48° is not the result of the structural change due to the electron irradiation but is due to the inherent nature of polyethylene single crystals—the setting angles reported so far range from 42° to 45° at room temperature: the radiation damage was thus not serious under these illumination conditions.

Hence, this method is useful and reliable in elucidating

fine structure such as the setting angle of the polyethylene molecule in the crystal. The application of the method to the electron diffraction pattern of various paraffin crystals allowed the setting angles of various paraffins to be measured. By comparing the data for polyethylene with those for paraffins, the nature of the setting angle in polyethylene and paraffin crystals has been revealed[24].

ACKNOWLEDGEMENT

The author is indebted to Professor Ken-ichi Katayama for his helpful discussions, Professor Natsu Uyeda for his valuable suggestions on the optical transform work and Dr Kazuo Ishizuka for his help with the computing.

REFERENCES

1 Frank, F. C. unpublished work; cf. Keller, A. *Polymer* 1962, **3**, 393
2 Geil, P. H. 'Polymer Single Crystals', John Wiley and Sons, New York, 1963
3 McMahon, P. E., McCullough, R. L. and Schlegel, A. A. *J. Appl. Phys.* 1967, **38**, 4127
4 Corradini, P., Petraccone, V. and Allegra, G. *Macromolecules* 1971, **4**, 770
5 Oyama, M., Shiokawa, K. and Ishimaru, T. *J. Macromol. Sci.* 1973, **B8**, 229
6 Bunn, C. W. *Trans. Faraday Soc.* 1939, **35**, 482
7 Kasai, N. and Kakudo, M. *Rep. Prog. Polym. Phys. Jpn.* 1968, **11**, 145
8 Zugenmaier, P. and Cantow, H. J. *Kolloid-Z.* 1969, **230**, 229
9 Kavesh, S. and Schultz, J. M. *J. Polym. Sci. A-2* 1970, **8**, 243
10 Iohara, K., Imada, K. and Takayanagi, M. *Polym. J.* 1972, **3**, 356
11 Kawaguchi, A., Uyeda, N. and Kobayashi, K., Paper presented at U.S. Japan Joint Seminar on Polymer Solid State, October 9–13, 1972, Cleveland, Ohio
12 Taylor, C. A. and Lipson, H. S. 'Optical transforms', Bell, London, 1964
13 Luis, J. and Amoros, M. 'Molecular Crystals', John Wiley and Sons, New York, 1969
14 Lipson, H. S. 'Optical Transforms', Academic Press, London, 1972
15 Klug, A. and DeRosier, D. J. *Nature* 1966, **212**, 29
16 Vainshtein, B. K. 'Structure Analysis by Electron Diffraction', Pergamon Press, Oxford, 1964
17 Cowley, J. M. and Moodie, A. F. *Acta Crystalogr.* 1959, **12**, 360
18 Dunkerley, B. D. and Lipson, H. S. *Nature* 1955, **176**, 81
19 Hindeleh, A. M. and Johnson, D. J. *Polymer* 1972, **13**, 423
20 Cowley, J. M. 'Diffraction Physics' North-Holland, New York, 1975
21 Dorset, D. L. *Acta Crystalogr.* 1976, **A32**, 207
22 Holland, V. F., Lindenmeyer, P. H., Trivedi, R. and Amelinckx, S. *Phys. State Sol.* 1965, **3**, 357
23 Kobayashi, K. and Sakaoku, K. *Lab. Invest.* 1965, **14**, 1096
24 Kawaguchi, A., Ohara, M. and Kobayashi, K. *J. Macromol. Sci.-Phys.* 1979, **B13**, 193